第25卷第1期
2006年2月

红外与毫米波学报
J. Infrared Millim. Waves

Vol. 25, No. 1
February, 2006

文章编号:1001-9014(2006)01-0001-05

MODIFICATION OF ABSORPTION SPECTRUM OF GaAs/AlGaAs QUANTUM WELL INFRARED PHOTODETECTOR BY POSTGROWTH ADJUSTMENT

Y FU[1], YANG Chang-Li[2]

(1. Theoretical Chemistry, Department of Biotechnology, Royal Institute of Technology, AlbaNova, S-106 91 Stockholm, Sweden;
2. East China Normal University, North Zhongshen Rd. 3663, 200062 Shanghai, China)

Abstract: Quantum well intermixing techniques modify the geometric shape of quantum wells to allow postgrowth adjustments. The tuning effect on the optical response property of a GaAs/AlGaAs quantum well infrared photodetector (QWIP) induced by the interdifussion of Al atoms was studied theoretically. By assuming an improvement of the heterointerface quality and an enhanced Al interdiffusion caused by postgrowth intermixings, the photoluminescence spectrum shows a blue-shifted, narrower and enhanced photoluminescence peak. The infrared optical absorption spectrum also shows the expected redshift of the response wavelength. However, the variation in the absorption peak intensity depends on the boundary conditions of the photo generated carriers. For high-quality QWIP samples, the mean free path of photocarriers is long so that the photocarriers are largely coherent when they transport across quantum wells. In this case, the enhanced Al interdiffusion can significantly degrade the infrared absorption property of the QWIP. Special effects are therefore needed to maintain and/or improve the optical properties of the QWIP device during postgrowth treatments.

Key words: quantum well infrared detector(QWIP); quantum well intermixing (QWI); boundary condition; optical absorption spectrum

CLC number: 0433.5+1 **Document code**: A

Introduction

Since 1980s, the infrared detector based on intersubband transitions in quantum well (QW) systems, called the quantum well infrared photoconductor (QWIP), has been studied and developed extensively and successfully [1]. Quantum well intermixing (QWI) techniques have become of great importance to modify the geometric shape of quantum wells, e.g., to induce the interdiffusion of Al atoms from the AlGaAs barriers to the GaAs wells in a GaAs/AlGaAs-based QWIP, for postgrowth adjustments on key physical parameters of the device, such as effective energy bandgap, optical absorption coefficient and refractive index. A number of QWI methods have been developed including SiO_2 capping followed by rapid thermal annealing [2], voltage tunable QWIPs [3~5], ion-implantation-induced intermixing [6~8], anodic-oxidation-induced intermixing [9], and other thermal treatments [10]. Selective QWI and thus selective modification of epitaxial structures are necessary for the fabrication of novel optoelectronic devices integrated into a single microchip. Selective area laser annealing of GaAs/AlGaAs QWIP material was investigated as a possible route towards the fabrication of two-color low-cost focal plane array devices [11].

The effectiveness of the QWI techniques has been demonstrated experimentally. However, it was constructed at the same time that the photocurrent was degraded, which was attributed by an enhanced alloy scattering due to the Al interdiffusion in GaAs/AlGaAs

Received: 2005-09-12, **revised date**: 2005-12-11 收稿日期: 2005-09-12, 修回日期: 2005-12-11

Foundation item: The project is partially supported by the National Natural Science Foundation of China (10474020)

Biography: Fu Ying (1964-), male, Jiangsu, China, Professor. Research fields is solid state physics and physics of nano electronics and photonics.

QWIP device which reduced the mobility of the photogenerated carriers [12]. Later, it was shown that the boundary conditions of the photogenerated carriers depend on the device structure and device operation condition [13,14]. In this paper, a further theoretical analysis is presented to study the effect of Al interdiffusion on the optical absorption property of the GaAs/AlGaAs QWIP by taking into account the boundary conditions of the photocarriers so that future QWI techniques can be properly designed. Section 1, 2 and 3 describe the basic QWIP structure and the theoretical analysis and discussions of its photoluminescence and infrared optical absorption property as functions of the Al interdiffusion. A brief summary is presented in Section 4.

1 Basic QWIP structure

We consider an n-type bound-to-continuum QWIP grown by molecular beam epitaxy on a [100] semi-insulating GaAs substrate. The QWIP contains fifty QWs sandwiched between 2.0-μm-thick top and 1.3-μm-thick bottom n^+ GaAs contact layers grown on a 0.5-μm-thick AlAs buffer layer. Each QW consists of nominally one 4.5-nm-thick Si-doped (10^{18} cm^{-3} GaAs quantum well and one 50-nm-thick undoped $Al_{0.3}Ga_{0.7}As$ barrier. During the postgrowth treatments, the as-grown sample is assumed to be ion-implanted and rapid thermal annealed, and then processed into standard QWIP device. The as-grown sample was characterized experimentally showing an photocurrent response peak at 8.0 μm [12].

By taking the z axis as the sample growth direction, the GaAs/AlGaAs QWIP heterostructure can be described in general by the degree of the Al interdiffusion given by Fick's diffusion equation

$$x(z) = \frac{x_0}{2}\left[2 + erf\left(\frac{z - W/2}{2L}\right) - erf\left(\frac{z + W/2}{2L}\right)\right] \quad , \tag{1}$$

where x_0 is the initial Al concentration in the barrier, W the quantum well width, L the Al diffusion length, and erf the error function. The center of the quantum well is taken as $z = 0$. Postgrowth process is expected to enhance the interdiffusion of Al atoms across the heterointerfaces, so that the QWI process is modelled theoretically by parameterizing the Al interdiffusion length L.

Knowing the Al distribution and the original doping profile we start the theoretical investigation by calculating the energy band structure in the self-consistent manner from Schrödinger and Poisson equations. Numerically it is shown that the Coulomb potential due to the ionized impurities and free-carrier re-distribution is negligibly small because of the low doping level in the AlGaAs quantum barriers and the almost-coincident spatial distributions of donors and free carriers in the GaAs quantum wells [15,16].

Theoretically we expect that the most prominent effect of the increased Al diffusion length is the lift-up of the ground sublevel in the GaAs quantum well due to the decrease of the quantum well width. The photoluminescence (PL) peak, corresponding to the intersubband transition between the ground electron-and hole-sublevels, is therefore expected to be blue shifted, and the cutoff wavelength of the infrared absorption peak due to the optical intra-subband transitions is to be redshifted, when the Al diffusion length is increased by the postgrowth activity.

2 Photoluminescence modification by Al interdiffusion

Comparison of the theoretical expectation with the PL measurement gives us a precise calibration for the Al atom diffusion length [12]. For an incident radiation in the form of $Ae^{i\omega t}$, by treating the weak electron-photon interaction as a perturbation and by the time-dependent perturbation theory, the transition probability per unit time is [17,18]

$$W(k,\hbar\omega) = \frac{e^2\hbar^2 n_{ph}\Gamma|\langle\Psi_{ek}a_0\cdot\nabla|\Psi_{hk}\rangle|^2}{m^{*2}\omega\varepsilon(\Omega_k - \hbar\omega)^2 + \Gamma^2} \quad , \tag{2}$$

where $\Omega_k = E_e + E_e(k) - E_h - E_h(k)$ is the excitation energy and is the photon energy, $\Psi_{ek}(r) = \psi_e(z)^{ik\cdot\rho}u_c(r)$ is the total wave function of conduction-band electron state $E_e + E_e(k)$, k and ρ are wave vector and spatial vector of the electron in the xy plane, $E_e(k)$ is the energy dispersion in the xy plane, $u_c(r)$ is the Bloch function. E_e is the eigenvalue of envelop function $\psi_e(z)$ along the z axis. n_{ph} is the photon density. The relationship between the photon density and the amplitude of the vector potential A is

$$|A|^2 = \frac{\hbar n_{ph}}{2\varepsilon\omega} \quad . \tag{3}$$

a_0 in Eq. (2) is the polarization of the incident radiation. Wave vector conservation during the excitation due to the translational symmetry in the xy plane is included in the above equation.

It is easy to show that

$$\langle \Psi_{ek} | a_0 \cdot \nabla | \Psi_{hk} \rangle = a_0 \cdot p_{cv} \langle \psi_e(z) | \psi_h(Z) \rangle \quad , \tag{4}$$

where $P_{cv} = \langle u_c(r) | \nabla | u_v(r) \rangle$ is the dipole moment. The total transition rate due to all contributing electrons, which determines the PL intensity, is then

$$W(\hbar\omega) = \int \frac{2dk}{(2\pi)^2} W(k, \hbar\omega) f_e[E_e + E_e(k)] f_h[E_h + E_{hk}(k)] \quad , \tag{5}$$

where the occupation of the conduction band sublevel is described by the Fermi function $f_e[E_e + E_e(k)]$ and the occupation of valence band sublevel is described by $f_h[E_h + E_h(k)]$. Under the weak optical excitation, the conduction-band electrons are described by a Fermi level E_f from the doping level in the quantum well

$$n_s = \frac{m_e^* (E_f - E_e)}{\pi\hbar^2} \quad , \tag{6}$$

at low temperature, where ns is the sheet doping density ($=4.5 \times 10^{11}$ cm^{-2} in the QWIP sample under investigation) and we have taken account the fact that there is only one confined sublevel, i. e., E_e, in the conduction band. The Fermi level of the valence-band holes is determined by the weak optical excitation power which is in the form of Boltzmann statistics.

In Eq. (2) Γ is the effective relaxation energy of carriers occupying the excited states. It represents the relaxation rate of the electrons from high-energy states back to the low-energy states. In practice the postgrowth process is expected to improve the quality of the samples so that Gamma becomes effectively reduced (Ref. [12] shows the increased alloy scattering during the photocarrier transportation across the QWIP device). By assuming the decrease of Γ and the increase of L as functions of the postgrowth activities, the calculated relationship between the PL spectrum and the postgrowth activity is presented in Fig. 1. Here we have included an exciton binding energy of 10.8 meV [19]. The energy bandgap of GaAs at 4.2 K is taken to be 1.519 eV, and other relevant material parameters are obtained from [20,21].

Fig. 1 shows that the PL peak is blue shifted due to the lift-up of the QW edges and the narrowing of the effective QWs. Moreover, due to the improvement of the heterointerfaces between GaAs QW and AlGaAs barriers, i. e., the decreasing of the relaxation energy, the full width at the half maximum of the PL peak decreases and the peak intensity increases. The results are largely confirmed experimentally, as can be expected.

3 Intrasubband optical spectrum

As can be concluded from the previous sub-section, we can determine the effective values of Γ and L from the experimental PL spectrum. After knowing the Al profile across the QWIP structure, we can calculate the absorption coefficient and then the photocurrent. The details of theoretical model and calculations were presented in Ref. [13,14]. With the parameters of Γ and L from Fig. 1, the resulting optical absorption spectra are presented in Fig. 2. Due to the lift-up of the QW edges and the narrowing of the QW widths, the ground sublevel is pushed up so that the optical excitation energy from the ground sublevel in the GaAs QW to the excited states above the AlGaAs conduction band edge decreases, resulting in the redshift of the absorption peak.

In Fig. 2 we have presented two sets of calculations using different boundary conditions for the photocarriers excited from the ground sublevel in the GaAs QW to the continuum states above the energy barrier of

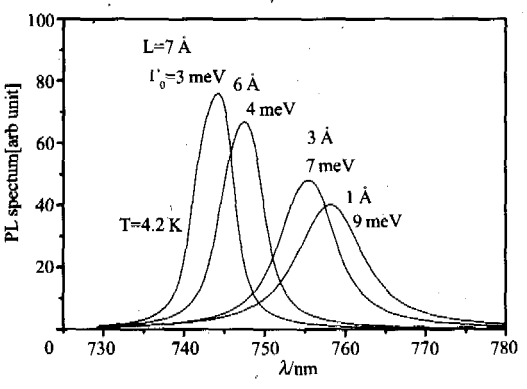

Fig. 1 Photoluminescence spectrum as a function of the Al diffusion length. $\Gamma = a - bL$, $a = 10.0$ meV and $b = 0.1$ meV/nm.

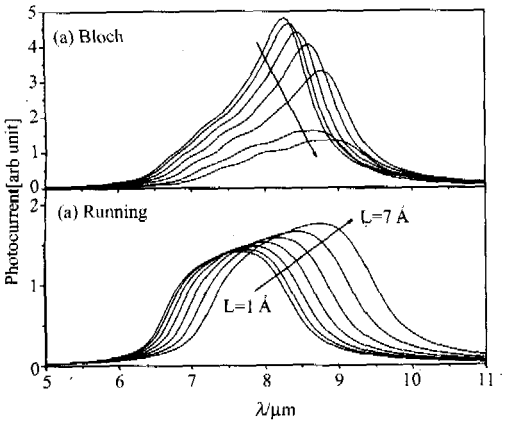

Fig. 2 Optical absorption coefficient. (a) Bloch-state boundary conditions apply to the photocarriers occupying the extended states in AlGaAs barriers. (b) Running-wave boundary conditions. The arrows indicate the increase of the Al diffusion length from 0.1 to 0.7 nm by a step of 0.1 nm, the corresponding Γ values are the same as in Fig. 1

AlGaAs layers [12], one is the running wave and the other one Bloch state. The Bloch-state boundary conditions mean that during the transport processes, the photocarriers are coherent across the whole QWIP structure. In Ref. [14] it was discussed that for QWIPs with wide quantum wells, the running-wave boundary conditions give a better fitting between theoretical and experimental optical spectra, whereas the Bloch-state boundary conditions apply to relatively narrow quantum wells. A clear key criterion concerning the appropriate boundary conditions is the mean free path of photogenerated carriers. When the mean free path is wider than the quantum wells, electron states of different quantum wells are coherently coupled so that Bloch-state boundary conditions apply (the AlGaAs quantum barriers are intentionally undoped so that the corresponding effective mean free path is large).

Fig. 2 therefore shows that for QWIPs where the photocarriers are coherent so that the Bloch-state boundary conditions apply, the postgrowth treatment not only redshifts the absorption peak, it also degrades the performance of the device by broadening the response spectrum as well as reducing the responsivity. For QWIPs where the running-wave boundary conditions apply, the postgrowth technique improves the responsivity of the device. Notice that the redshift of the responding peak is smaller when the Bloch-state boundary conditions apply.

The reality can be much complicated. With the ion implantations or other postgrowth processes studied in the present work, the increased diffusion length makes the effective QW width wider, resulting in a transition from Bloch-state to running-wave boundary conditions if the Bloch-state boundary conditions apply before the postgrowth treatment and the increase of the effective QW width is large enough. On the other hand, the expected improvement in the sample quality means an increased coherence of the excited states due to the reduced relaxation energy, by which we will expect a transition from running-wave to Bloch-state boundary conditions if the running-wave boundary conditions apply originally and the increment in the coherence is sufficient.

Since the redshift of the response wavelength is small for Bloch-state boundary conditions, a decrease in the variation of the QWIP's response wavelength as a function of the postgrowth activity can be induced due to the changes of the boundary conditions for photocarriers.

We can therefore propose the following way to study the effectiveness of the postgrowth technique in improving the device performance of the QWIP: Γ and L values are first determined from the experimental PL spectrum. The coherence of the photocarriers is then to be determined by monitoring carefully the variation of the response wavelength during the postgrowth treatment. When photocarriers are determined to be coherent, QWI activity should be limited in order to maintain the QWIP device performance. It must also be noticed however that the responsivity of the coherent QWIP is in general much better than the running-wave QWIP, as can be concluded from the comparison of the optical absorption spectra in Fig. 2.

4 Conclusion

Intersubband GaAs/AlGaAs quantum well infrared photodetector (QWIP) technology has been successfully developed together with the advancing developments of quantum well intermixing techniques for postgrowth adjustment of the device structures.

By assuming an improvement in the heterointerface quality and an enhanced Al interdiffusion due to

the postgrowth intermixing, the photoluminescence spectrum shows a blue-shifted, narrower and enhanced photoluminescence peak. The infrared optical absorption spectrum also shows the expected red-shift. However, we have demonstrated theoretically by this work that the variation in the responsivity of the QWIP device depends on the boundary conditions of the photogenerated carriers occupying the extended states above the AlGaAs potential barrier. For high-quality QWIP samples, the mean free path of photocarriers is long so that the photocarriers are largely coherent while transporting across quantum wells. In this case, the enhanced Al interdiffusion can significantly degrade the infrared absorption capability of the QWIP device. Special effects are therefore needed to maintain and/or improve the optical properties of the QWIP device during postgrowth treatments.

REFERENCES

[1] Lu W, Fu Y. *Quantum well infrared detectors, in Encyclopedia of Nanoscience and Nanotechnolgy* [M]. (ed. H. S. Nalwa), New York: American Scientific Publishers, 2004, **9**:179—197.

[2] Chi J Y, Wen X, Koteles E S, *et al.* Spatially selective modification of GaAs/AlGaAs quantum wells by SiO_2 capping and rapid thermal annealing [J]. *Appl. Phys. Lett.*, 1989,**55**:855—857.

[3] Tidrow M Z, Choi K K, Farley C W, *et al.* Multicolor infrared detection using a voltage tunable bandpass filter [J]. *Appl. Phys. Lett.*, 1994,**65**:2996—2998.

[4] Chiang J-C, Li S S, Tidrow M Z, *et al.* A voltage-tunable multicolor triple-coupled InGaAs/GaAs/AlGaAs quantum-well infrared photodetector for 8 - 12 μm detection [J]. *Appl. Phys. Lett.*, 1996,**69**:2412—2414.

[5] Bandara S V, Gunapala S D, Liu J K, *et al.* 10 - 16 μm Broadband quantum well infrared photodetector [J]. *Appl. Phys. Lett.* 1998,**72**:2427242—9.

[6] Redinbo G F, Craighead H G, Hong J M. Proton implantation intermixing of GaAs/AlGaAs quantum wells [J]. *J. Appl. Phys.* 1993,**74**:3099—3102.

[7] Johnston M B, Cal M, Li N, *et al.* Interdiffused quantum-well infrared photodetectors for color sensitive arrays [J]. *Appl. Phys. Lett.*, 1999,**75**: 923—925.

[8] Fu L, Tan H H, Jagadish C, *et al.* Tuning the detection wavelength of quantum-well infrared photodetectors by single high-energy implantation[J]. *Appl. Phys. Lett.*, 2001,**78**: 10—12.

[9] Yuan S, Kim Y, Tan H H, *et al.* Anodic-oxide-induced interdiffusion in GaAs/AlGaAs quantum wells [J]. *Appl. Phys. Lett.*, 1998,**83**:1305—1311.

[10] Feng W, Chen F, Cheng W Q, *et al.* Influence of growth conditions on Al-Ga interdiffusion in low-temperature grown AlGaAs/GaAs multiple quantum wells [J]. *Appl. Phys. Lett.*, 1997,**71**:1676—1678.

[11] Dubowski J J, Song C Y, Lefebvre J, *et al.* Laser-induced selective area tuning of GaAs/AlGaAs quantum well microstructures for two-color IR detector operation [J], *J. Vac. Sci. Technol.*, 2004, **A22**:887—890.

[12] Fu Y, Willander M. Alloy scattering in GaAs/AlGaAs quantum well infrared photodetector [J]. *J. Appl. Phys.*, 2000,**88**:288—292.

[13] Fu Y. Boundary conditions of continuum states in characterizing photocurrent of GaAs/AlGaAs quantum well infrared photodetector [J]. *Superlattices and Microstructures.* 2001, **30**: 69—74.

[14] Fu Y, Willander M, Jiang J, *et al.* Photocurrents of 14 μm quantum-well infrared photodetectors [J]. *J. Appl. Phys.* 2003,**93**:9432—9436.

[15] Fu Y, Willander M, Li N, *et al.* Quantum mechanical model and simulation of GaAs/AlGaAs quantum well infrared photodetector-I Optical aspects [J]. *J. Infrared Millim. Waves*, 2002,**21**(4):321—326.

[16] Fu Y, Willander M, Li N, *et al.* Quantum mechanical model and simulation of GaAs/AlGaAs quantum well infrared photodetector-Ⅱ Electrical aspects [J]. *J. Infrared Millim. Waves*, 2002,**21**(5):401—407.

[17] Böer K W. *Survey of Semiconductor Physics* [M]. New York: Van Nostrand Reinhold. 1990:325—354.

[18] Ridley B K. *Quantum Processes in Semiconductors* [M]. Britain: Oxford Clarendon Press. 1988:184—234.

[19] Fu Y, Chao K A. Exciton binding energy in GaAs/AlGaAs multiple quantum wells [J]. *Phys. Rev.*, **B43**: 12626—12629.

[20] Madelung O. *Semiconductors Group Ⅳ Elements and Ⅲ-Ⅴ Compounds* [M]. Berlin: Springer-Verlag, 1991.

[21] Vurgaftman I, Meyer J R, Ram-Mohan L R. Band parameters for Ⅲ-Ⅴ compound semiconductors and their alloys [J]. *J. Appl. Phys.* 2001,**89**:5815—5875.